



OPEN

Comfort evaluation of ZnO coated fabrics by artificial neural network assisted with golden eagle optimizer model

Nesrine Amor^{1✉}, Muhammad Tayyab Noman¹, Michal Petru¹ & Neethu Sebastian²

This paper introduces a novel technique to evaluate comfort properties of zinc oxide nanoparticles (ZnO NPs) coated woven fabrics. The proposed technique combines artificial neural network (ANN) and golden eagle optimizer (GEO) to ameliorate the training process of ANN. Neural networks are state-of-the-art machine learning models used for optimal state prediction of complex problems. Recent studies showed that the use of metaheuristic algorithms improve the prediction accuracy of ANN. GEO is the most advanced metaheuristic algorithm inspired by golden eagles and their intelligence for hunting by tuning their speed according to spiral trajectory. From application point of view, this study is a very first attempt where GEO is applied along with ANN to improve the training process of ANN for any textiles and composites application. Furthermore, the proposed algorithm ANN with GEO (ANN-GEO) was applied to map out the complex input-output conditions for optimal results. Coated amount of ZnO NPs, fabric mass and fabric thickness were selected as input variables and comfort properties were evaluated as output results. The obtained results reveal that ANN-GEO model provides high performance accuracy than standard ANN model, ANN models trained with latest metaheuristic algorithms including particle swarm optimizer and crow search optimizer, and conventional multiple linear regression.

Zinc oxide (ZnO) is an inorganic compound used in various products and applications including food supplements, cosmetics, plastics, textiles, ceramics, paints, batteries and many more. ZnO in nanoforms is available in different dimensions and morphologies including nanoparticles, nanowires, nanosheets and nanoflowers. ZnO nanoparticles (ZnO NPs) are widely used in photocatalysis, self-cleaning and antimicrobial applications^{1–3}. The use of ZnO for thermophysiological and sensorial comfort is also significant from different aspects. Thermophysiological properties are influential parameters that play important role in the evaluation of fabric comfort⁴. In a recent study, Noman *et al.* synthesized and coated ZnO NPs on woven textiles by sonication and practically evaluated thermal resistance, heat flow, thermal diffusivity, accumulative One-way transport index and wetting time⁵. In this extended study, a prediction model is designed based on the application of a latest machine learning algorithm (GEO) and its synchronization with ANN in order to improve the training process of ANN. The benefit of using ANN in this work, is the adaptation of existing relationship without any physical mechanism. The resulted ANN-GEO model works in three ways i.e., correlates the actual response with the process variables, analyses the predicted response of each variable and indicates the better approach.

ANN is an efficient machine learning tool suitable for the prediction of output response when input conditions are not defined^{6–8}. Khude *et al.* used ANN with adaptive network-based fuzzy inference system (ANFIS) for antimicrobial evaluation of knitted fabrics. The results reveal that ANFIS performed better under small number of data sets⁹. Knanat *et al.* applied standard ANN for the evaluation of thermal resistance of knitted fabrics. Two different models of ANN were developed based on input conditions. The results of both models showed excellent prediction of thermal resistance¹⁰. Lu *et al.* combined ANN with multiple linear regression (MLR) for tensile strength of wool fibers. A high correlation was observed between actual and predicted values. However, ANN showed higher accuracy and lower error than MLR¹¹. In a study, Malik *et al.* applied ANN for comfort evaluation of woven fabrics. ANN was trained with feedforward back propagation composed of Bayesian regularization and Levenberg-Marquardt functions. The results showed that ANN adjusts the data sets with lower mean absolute

¹Technical University of Liberec, 461 17, Studentská 1402/2, Liberec 1, Czech Republic. ²Institute of Organic and Polymeric Materials, National Taipei University of Technology, No. 1, Section 3, Zhongxiao East Road, Taipei 106, Taiwan, ROC. ✉email: nesrine.amor@tul.cz

error (MAE)¹². In another work, Malik *et al.* used ANN for loom parameters and fabric properties including porosity, pore size and air permeability. The obtained results showed that ANN is an excellent prediction tool with minimum error¹³. Wong *et al.* combined ANN with fuzzy logic (FL) for clothing comfort and results reveal better correlation of input and out conditions¹⁴. Mishra applied ANN to predict yarn strength. Selected variables were yarn count, yarn crimps and yarn strengths in both longitudinal and transverse directions. The results reveal a percentage increase in both directions¹⁵.

In an experimental study, El-Geiheini *et al.* investigated yarn types and applied ANN for yarn tenacity and elongation. The results showed ANN is suitable for the evaluation of various properties with minimum error¹⁶. In another study, Erbil *et al.* applied ANN and regression for tensile strength of rotor yarns. ANN was trained with Levenberg-Marquardt backpropagation. In addition, a comparison of ANN and regression was performed for prediction efficiency. The results demonstrated that ANN gives better prediction output than regression¹⁷. Breuer *et al.* applied ANN for short fiber composites under representative volume element database. The elastic properties of short fiber reinforced plastics were evaluated and results showed that ANN predicts the stiffness in good manner¹⁸. Wang *et al.* used ANN to predict the tensile strength of ultrafine glass fiber felts. The results are modelled with mean diameter, bulk density and resin content. ANN simulation showed high prediction accuracy with low mean relative errors¹⁹. Farook *et al.* used ANN for cotton fibre maturity. The results showed low error for ANN²⁰. Unal *et al.* used ANN and regression for single jersey knitted fabrics to predict air permeability and bursting strength of knit structures. Simulation results showed that both methods were good for prediction²¹. Farooq *et al.* applied ANN for shade change prediction of dyed knitted fabrics. The observed results showed that ANN provides high prediction accuracy for shade change²². Recently, Amor *et al.* applied ANN and MLR on functional properties of nano TiO₂ coated composites. Simulation results showed that for prediction accuracy, ANN outperformed MLR²³. In another study, Amor *et al.* used deep neural network (DNN) for the prediction of methylene blue removal. DNN model showed better results than MLR²⁴. The literature discussed above reveal that multilayer perceptron (MLP) is a popular class of feedforward ANN model, and extensively used ANN algorithm in textiles and composites industries²⁵.

The application of metaheuristic algorithms (particle swarm optimizer, genetic algorithm, crow search optimizer) for accuracy improvement of ANN has gained considerable attention. Genetic algorithm (GA) was used with ANN to improve pilling performance²⁶, yarn tenacity²⁷, ultraviolet protection factor (UPF)²⁸. Grey wolf optimizer (GWO) was combined with ANN to detect and predict the coating thickness by hyperspectral images²⁹. ANN trained with particle swarm optimization (PSO) used for thermal properties³⁰ and trained with crow search algorithm (CSA) used for the prediction of functional properties of nanocomposites³¹. Recently, a novel nature-inspired metaheuristic algorithm known as GEO, has been introduced to solve global optimization. GEO is inspired by the intelligence of golden eagles for hunting by tuning their speed according to the spiral trajectory. GEO is distinguishable from GA, PSO, CSA and dragonfly algorithm (DA) by its setting parameters that make the process more intuitive and effective in solving complex problems³². In addition, the application of GEO in real-world applications showed its potential and suggested its use in other fields especially textiles and polymer composites.

This study provides the following benefits: (1) Proposing the use of GEO to train MLP. (2) Investigating the accuracy of propose ANN-GEO for the prediction of comfort properties of ZnO coated fabrics by creating a relationship between ZnO, comfort properties and ultrasonic irradiations. The amount of ZnO NPs, fabric mass and fabric thickness were selected as input variables and comfort properties i.e., thermal diffusivity, thermal resistance, heat flow, accumulative One-way transport index and wetting time were considered as output responses. (3) Comparing the performance of ANN-GEO with standard ANN, standard MLR and ANN trained by PSO, CSA and GA algorithms.

Material and methods

Materials. Two types of plain weave woven fabric (100% cotton and polyester) were used for samples preparation. Chemicals i.e., sodium hydroxide, zinc chloride and ethanol were received from sigma aldrich. The variables selected for this study were ZnO NPs coated amount, fabric mass measured as gram per square meter (GSM) and fabric thickness before and after treatment. The combination of these variables is described in Table 1.

Conditioning. Before any treatment, all the samples were conditioned at temperature i.e., 23 ± 2 °C and relative humidity i.e., 65 ± 2 for one day according to ASTM standard D 1776-16. After that, fabric mass was calculated by ASTM D 3776. ASTM D 1777-96 (2019) standard was used to measure fabric thickness before and after the application of ZnO NPs.

Application of ZnO NPs. Synthesis and coating of ZnO NPs were performed on all the samples according to the procedure as reported in our previous studies^{33,34}. Fabric samples were individually immersed in water and then different amount of ZnCl₂ was added. Later on, NaOH in granular form was added. In order to complete the reaction, sonication was applied for 1 h. After sonication, samples were squeezed on padder and dried in an oven. ZnO NPs were characterised for their morphology and topography. Ultrahigh resolution scanning electron microscopy (UHR-SEM) was used to characterise the morphological and topographical changes. ZnO NPs coated amount was calculated by inductively coupled plasma atomic emission spectroscopy (ICP-AES).

Artificial neural network. Prediction of thermophysiological properties of ZnO NPs coated samples is a challenging task due to the complex relationship between applied chemicals and obtained results. ANN has achieved important milestones in the field of artificial intelligence (AI)³⁵. ANN models are inspired by biological neural networks that allow them to capture linear or nonlinear complex relationships between dependent

Sample	ZnO NPs coated amount [ppm]	GSM [gm^2]	Thickness [mm]
1	–	110	0.25
2	581	115	0.31
3	1090	118	0.38
4	–	224	0.66
5	598	229	0.72
6	1110	233	0.77
7	–	118	0.32
8	493	124	0.36
9	1032	128	0.41
10	–	230	0.66
11	583	234	0.78
12	1096	238	0.84

Table 1. The input variables for experimental design.

and independent variables³⁶. It includes large groups of neurons connected by axons. The artificial neuron has multiple inputs that are weighted, summed up and followed by an activation function or transfer function. Every neuron receives input from various sources and applies activation function to provide the desired results. The advantages of ANN are exploration, creation and derivation of new data through training process³⁷.

MLP is a feedforward ANN model in which one direction processes the information from input to output neurons under multiple hidden layers. MLP deals with non-linear models by decreasing the targeted error by tailoring weight and biases³⁸. In MLP, training process is implemented in four steps: 1) Initialization: assuming that there is no prior information available and initializing the weights and thresholds values. 2) Forward propagation: the inputs of ANN model are the experimental data and their effects propagate at different stages by moving forward the network layer by layer which creates the network output. 3) Error computation: the error vector is calculated by actual and predicted output difference. 4) Backward propagation: the calculated error vector propagates backwards and synaptic weights are adjusted.

Generally, ANN is used to predict the output variables $y = [y_1, \dots, y_m]$ for a given set of input variables $x = [x_1, \dots, x_k]$ from their training values. The results depend on weights $w = [w_1, \dots, w_k]$. The relationship between input and output of ANN model is presented in the following equation^{39,40}:

$$y = \varphi \left(\sum_i w_i * x_i + b \right) \quad (1)$$

where, y represents the desired output. x_i represents the selected i^{th} input. w_i represents the i^{th} weight and b is the bias. φ represents the activation function. More theoretical detail of ANN models with their training algorithms is provided by various researchers^{41–45}. In the ANN model, by increasing the number of network layers, the results will be significantly more accurate. However, this increase will make the training process more difficult to fit and will lead to a time-consuming process. We, therefore, adopted the classical structure of feedforward ANN (MLP model) in the present work. The classical structure of feedforward ANN consists of three layers (one input layer, one output layer and one hidden layer). Figure 1 illustrates the schematic ANN model for this study.

The recommended quantity to train the network, is from 60% up to 90% of the samples⁴⁶. The datasets of Table 1 were divided into three parts (training, validation and testing) for the proposed ANN model, where 60% of total data was used to train the network, 15% was used for validation and remaining 25% was used for testing. Once the training process is completed, the developed model is validated for unseen data during training. Random sub-sampling cross-validation method was applied to evaluate the topology and training of proposed model. The training inputs vectors are shown in Table 1. The output vectors include thermal resistance, thermal diffusivity, heat flow, accumulative One-way transport index and wetting time. The selected number of input and output nodes were 3 and 5 respectively.

ANN optimized with golden eagle optimizer.

- **Golden eagle optimizer**

GEO is a new metaheuristic method that was introduced very recently to solve global optimization problems. GEO algorithm is inspired and mathematically modeled by the intelligence of the golden eagles based on controlling the speed of their spiral track. Golden eagle is a special kind of swarm that has a greater propensity to cruise around and search for prey at the start of hunt. By controlling these two components, i.e., cruise propensity and attack propensity, GEO is quickly able to hunt the best available prey in the feasible area.

The golden eagle in cruising and hunting has a unique feature i.e., occurs in a spiral trajectory which means that prey is generally on one side of the eagle. This enables them to control target prey carefully and boulders

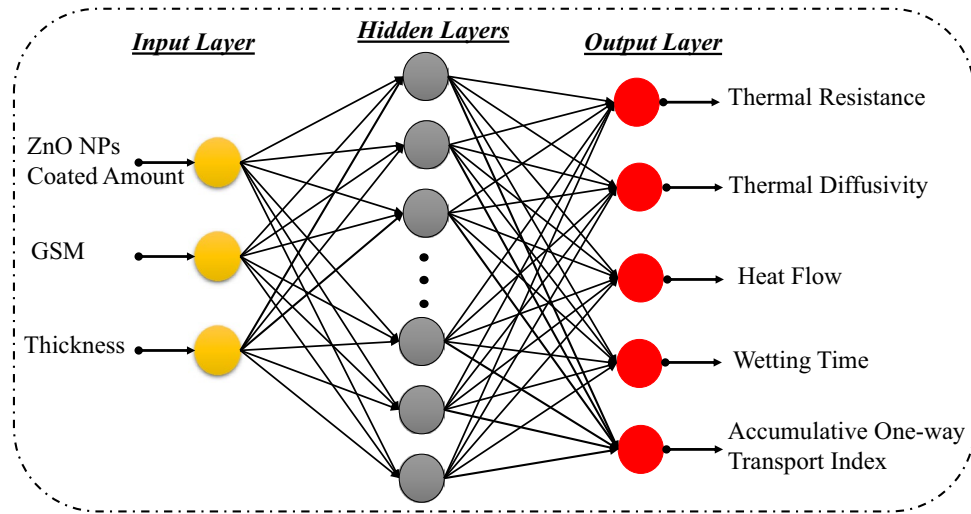


Figure 1. ANN model for the prediction of comfort properties of ZnO coated fabrics.

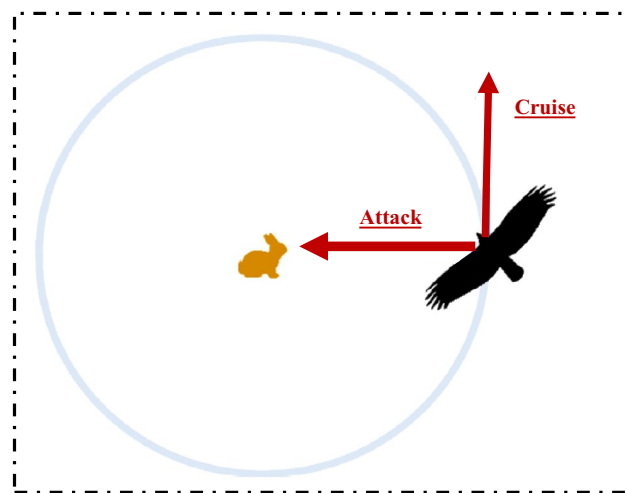


Figure 2. Spiral movement of golden eagles³².

to find a suitable angle of attack. At the same time, they check other areas for better food. The hunting method of golden eagles mainly depend on the following feature: they have an intelligent memory that allows them to memorize the propensity for both cruise and attack during the flight.

The mathematical formulations of golden eagles to mimic the movements for searching the prey are mainly described by:

- **The spiral movement of golden eagles:** In GEO, every golden eagle keeps in its memory the best visited position so far. The eagle has an attraction towards the cruise and towards attacking the prey simultaneously to search for better food. Figure 2 depicts the cruise and attack vectors in 2D space. At every iteration, every golden eagle j can randomly chooses a prey that has been caught by another golden eagle l and circles around the best position visited by golden eagle l so far. The golden eagle j also has the feature of selection to circle its own memory; thus, we have $l \in \{1, 2, \dots, N_{GE}\}$, where N_{GE} represents the number of golden eagles.
- **Prey selection:** At every iteration, every golden eagle should select a prey to carry out the cruise and attack operations. In addition, each golden eagle chooses the desired prey from the memory of the whole flock. Therefore, the cruise and attack vectors are computed according to the selected prey. After that, it checks its memory If the new location is better than the previous location, then the memory is updated with the new finding.
- **Attack:** The attack can be described using a vector starting from the actual position of golden eagle j and ending in the position of the prey in the eagle's memory, as follows:

$$\vec{A}_j = \vec{X}_l^* - \vec{X}_j, \tag{2}$$

where \vec{A}_j represents the attack vector of golden eagle j , \vec{X}_1^* represents the best position visited by eagle l so far, and \vec{X}_j represents the current position of eagle j .

- **Cruise:** The cruise vector is a perpendicular vector to the attack vector and tangent to the circle. It is also known as linear speed of golden eagle to attack the prey. The destination point on the cruise vector is given below:

$$\vec{C}_j = \frac{d - \sum_{f \neq j} a_f}{a_j} \tag{3}$$

where, d represents the hyperplane equation in n -dimensional space, $a_j, a_f \in \vec{A}_j$, where $\vec{A}_j = [a_1, a_2, \dots, a_n]$ is the attack vector.

- **Moving to new positions:** Moving to new positions of the golden eagles are mainly depends on the attack and cruise vectors. Therefore, the step vector of golden eagle j in iteration t is presented by the following equation:

$$\Delta_{x_j} = \vec{r}_1 p_a \frac{\vec{A}_j}{\|\vec{A}_j\|} + \vec{r}_2 p_c \frac{\vec{C}_j}{\|\vec{C}_j\|} \tag{4}$$

where p_a^t represents the attack coefficient at iteration t and p_c^t represents the cruise coefficient at iteration t and control how the golden eagles are affected by cruise and attack. \vec{r}_1 and \vec{r}_2 are a random vectors.

The new position of the golden eagle is then given by:

$$x_j^{t+1} = x_j^t + \Delta_{x_j} \tag{5}$$

If the fitness function j provides better than the previous positions, then its memory will be updated with the new position.

- **Transition from exploration to exploitation:** GEO algorithm uses the attack coefficient p_a and the cruise coefficient p_c to switch from the state of exploration to the state of exploitation. p_a and p_c can be computed using the following linear expressions:

$$p_a = p_a^0 + \frac{t}{T} |p_a^T - p_a^0| \tag{6}$$

$$p_c = p_c^0 + \frac{t}{T} |p_c^T - p_c^0| \tag{7}$$

where p_a^0 and p_c^0 are, respectively, the initial values for propensity to attack p_a and for propensity to cruise p_c , t represents the current iteration, T is the maximum number of iterations, p_a^T and p_c^T are, respectively, the final values for propensity to attack p_a and for propensity to cruise p_c .

- **Optimized ANN model with golden eagle optimizer**

The main inconvenient of ANN algorithm is that it can get stuck in local minimums easy and has a slow convergence rate. In recent years, researchers have shown that incorporating metaheuristics methods like GA⁴⁷ and PSO⁴⁸⁻⁵⁰ in ANN, improves the performance of training process and the convergence rate significantly. However, GEO algorithm has been never used and investigated in training ANN. Training process involves identifying the corresponding set of influences that reduce the training error. Therefore, we proposed a new combined model that integrates GEO algorithm in the training of ANN to improve the prediction efficiency of ZnO NPs coated fabrics for thermophysiological properties. In this framework, ANN model is optimized by GEO algorithm in order to optimize the threshold and the weight, that significantly improves the prediction accuracy of the desired output. The flowchart of the proposed ANN-GEO model for comfort evaluation is presented in Fig. 3.

In ANN-GEO algorithm, at each iteration t , the golden eagle position $x^{j,t+1}$ is considered as the collection of weights. The MSE between the actual and predicted outputs is considered as the fitness function of ANN-GEO algorithm, where GEO seeks to minimize it during the ANN training process. Therefore, the fitness function is described by the following expression:

$$\text{Minimize}\{F\} = \min\left\{\frac{1}{N} \sum_{j=1}^N \sum_{i=1}^n (y_{ji} - \hat{y}_{ji})^2\right\} \text{ where } j = 1, \dots, M \text{ and } i = 1, \dots, N. \tag{8}$$

where, M is the the number of training samples and N is the number of output nodes.

The proposed ANN-GEO algorithm is mainly based on the following steps:

1. Initialization of the parameters of ANN-GEO algorithm: Golden eagle includes all weights and thresholds of ANN network i.e., connection weight for input and hidden layers, threshold for hidden layer, connection weight for hidden output layers, and threshold of output layer.
2. Initialization of memory, position, propensity to attack p_a as well as propensity to cruise p_c for every golden eagle: ANN-GEO initiates with random initialization of golden eagle positions where every golden eagle moves into the weighted search space.

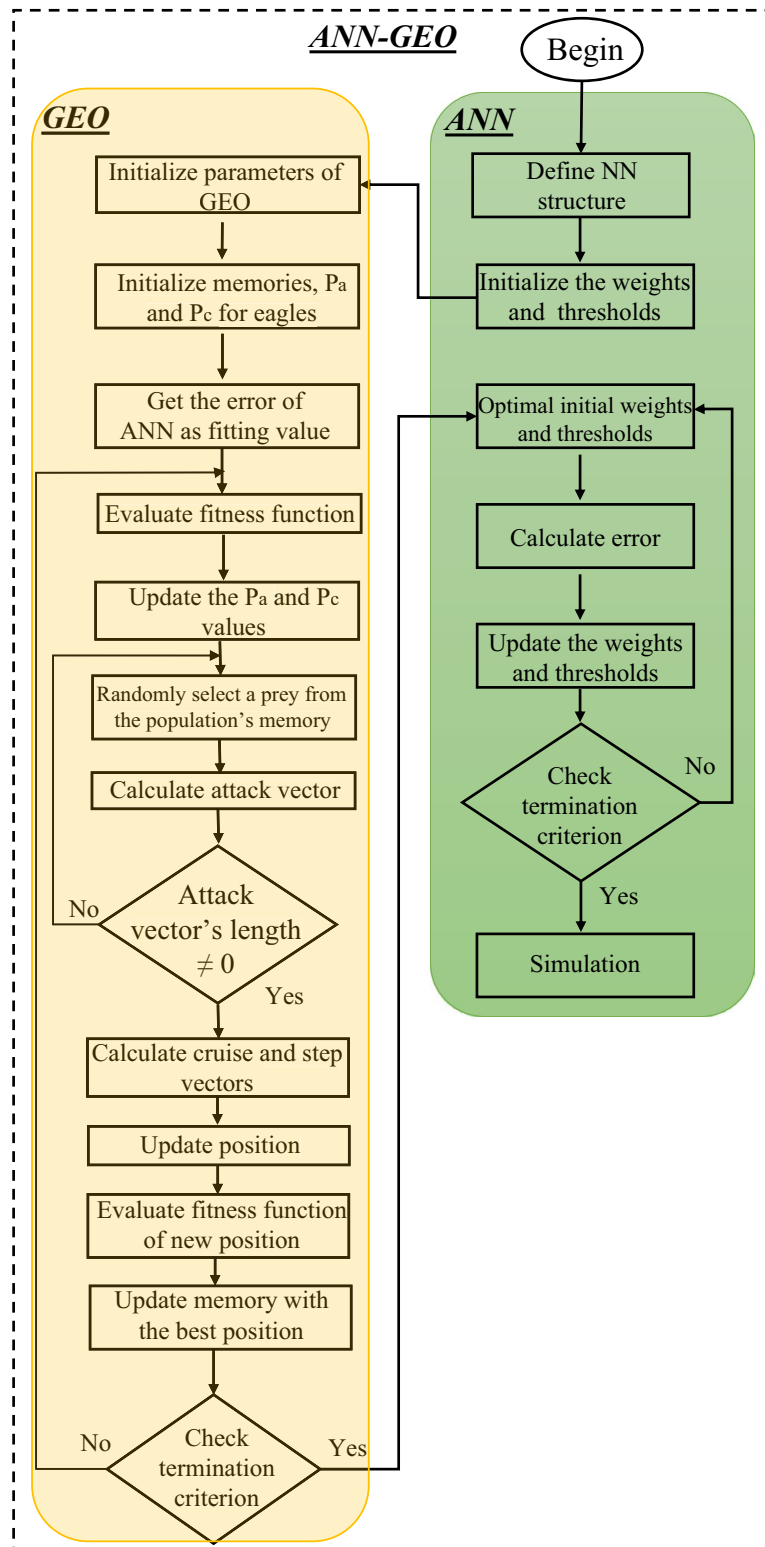


Figure 3. ANN-GEO model for the prediction of thermophysiological comfort properties of ZnO NPs coated fabrics.

3. Measurement of fitness function: Here, initial weights and bias are used to estimate initial training error.
4. Compute the attack vectors: Update the p_a and p_c values, and randomly select a prey. Then, computes attack vectors using Eq. (2).

5. Calculate the cruise and step vectors using Eqs. (3) and (4), respectively.
6. Compute the new position of the golden eagle using Eq. (5).
7. Estimate fitness function for new position, update p_a and p_c using Eqs. (6) and (7), respectively, and update memories of all golden eagles with best positions, and so on until the end of iterations.

Robustness and sensitivity analysis. Prediction performance of thermophysiological comfort properties of ZnO NPs coated fabrics using ANN-GEO was estimated using statistical methods e.g., mean squared error (MSE), mean absolute error (MAE), root mean squared error (RMSE) and correlation coefficient (R), which are defined below.

$$MAE = \frac{1}{m} \sum_{j=1}^m |y_j - \hat{y}_j|, \quad (9)$$

$$MSE = \frac{1}{m} \sum_{j=1}^m (y_j - \hat{y}_j)^2, \quad (10)$$

$$RMSE = \sqrt{\frac{1}{m} \sum_{j=1}^m (y_j - \hat{y}_j)^2}, \quad (11)$$

$$R = \frac{\sum_{j=1}^m (y_j - \bar{y})(\hat{y}_j - \bar{\hat{y}})}{\sqrt{\sum_{j=1}^m (y_j - \bar{y})^2} \sqrt{\sum_{j=1}^m (\hat{y}_j - \bar{\hat{y}})^2}}. \quad (12)$$

where y_j and \hat{y}_j are, respectively, the actual and predicted thermophysiological comfort properties. m represents the number of samples. \bar{y} is the computed average of the actual properties and $\bar{\hat{y}}$ represents the computed average of the predicted properties.

The proposed model ANN-GEO was statistically tested using one-way ANOVA to evaluate its efficacy and durability comparing to others methods for the prediction of the thermophysiological comfort properties. ANOVA is an independent statistical approach to verify the statistical significance between inputs and outputs^{51–53}. ANOVA uses F ratio to check the existence of any significant difference between the outputs.

Results and discussion

SEM and ICP-AES analysis. UHR-SEM was used for surface topography and morphology evaluation of treated and untreated samples as illustrated in Fig. 4. UHR-SEM images were taken at magnification 5k x and 50k x for cotton and at 250 x and 10k x for polyester respectively. A clean and smooth surface of untreated cotton and polyester can be observed in Fig. 4a,d respectively. A quasi spherical shape with homogeneous distribution of ZnO NPs was observed for both type of fabrics. In addition, ICP-AES analysis confirmed the presence of ZnO NPs on both fabrics. However, no traces were detected on untreated samples.

Comfort properties of ZnO NPs coated fabrics were determined through ANN under golden eagle optimizer (ANN-GEO). The obtained simulation results of ANN-GEO model were compared with standard ANN model, optimized ANN model with particle swarm optimization (ANN-PSO), optimized ANN model with genetic algorithm (ANN-GA) and optimized ANN model with crow search algorithm (ANN-CSA).

Parameters setting of the optimized ANN models with metaheuristics algorithms The proposed ANN model has three-layers i.e., an input layer, a hidden layer, and an output layer. After several trials, we found that the network provides highly accurate results with 9 hidden layer nodes, thus we considered that the number of hidden layer nodes for all proposed algorithms to be 9. The settings of training parameters of ANN, optimized models with GEO, PSO, CSA, and GA are introduced in Table 2.

Comparison of ANN-GEO with currently used ANN-metaheuristics The predicted values of comfort properties of ZnO NPs coated fabrics under standard ANN, ANN-GEO, ANN-PSO, ANN-GA and ANN-CSA are presented in Fig. 5, where predicted results for thermal resistance, thermal diffusivity, heat flow, wetting time and accumulative One-way transport index are presented from first row to fifth row respectively. We performed several trials with different number of populations (i.e., number of crows, number of swarm, etc) in each proposed algorithm in order to confirm a fair comparison between all applied algorithms. Then, we selected the best results with higher accuracy and lower errors for the prediction of comfort properties of ZnO NPs coated fabrics in each algorithm. For the stochastic nature of ANN-GEO, ANN-CSA, ANN-PSO, ANN-GA and ANN models, the prediction procedure of every property is repeated 1000 times and an average of 1000 times prediction is taken.

The values of prediction errors MAE, MSE, RMSE as well as the coefficient of correlation R between predicted and actual values for all evaluated comfort properties using ANN-GEO, ANN-GA, ANN-PSO, ANN-CSA and ANN are shown in Fig. 6 for thermal resistance, Fig. 7 for thermal diffusivity, Fig. 8 for heat flow, Fig. 9 for wetting time and Fig. 10 for accumulative One-way transport index respectively. We observed that ANN-GEO has lower prediction errors and higher prediction accuracy according to the coefficient of correlation ($R \approx 1$) for all evaluated outputs. The proposed ANN-GEO model significantly outperformed ANN-GA, ANN-PSO, ANN-CSA and standard ANN in both training and testing processes. Another observation found that ANN-PSO provides very good prediction accuracy than ANN-CSA, ANN-GA and standard ANN for comfort properties. However, ANN-CSA prediction results have the lower accuracy with higher prediction error.

The average time of each run for thermal resistance in GEO algorithm is 0.232 s, in PSO is 0.316 s, in GA is 0.322 s and in CSA is 0.689 s. The average time of each run for thermal diffusivity in GEO algorithm is 0.187

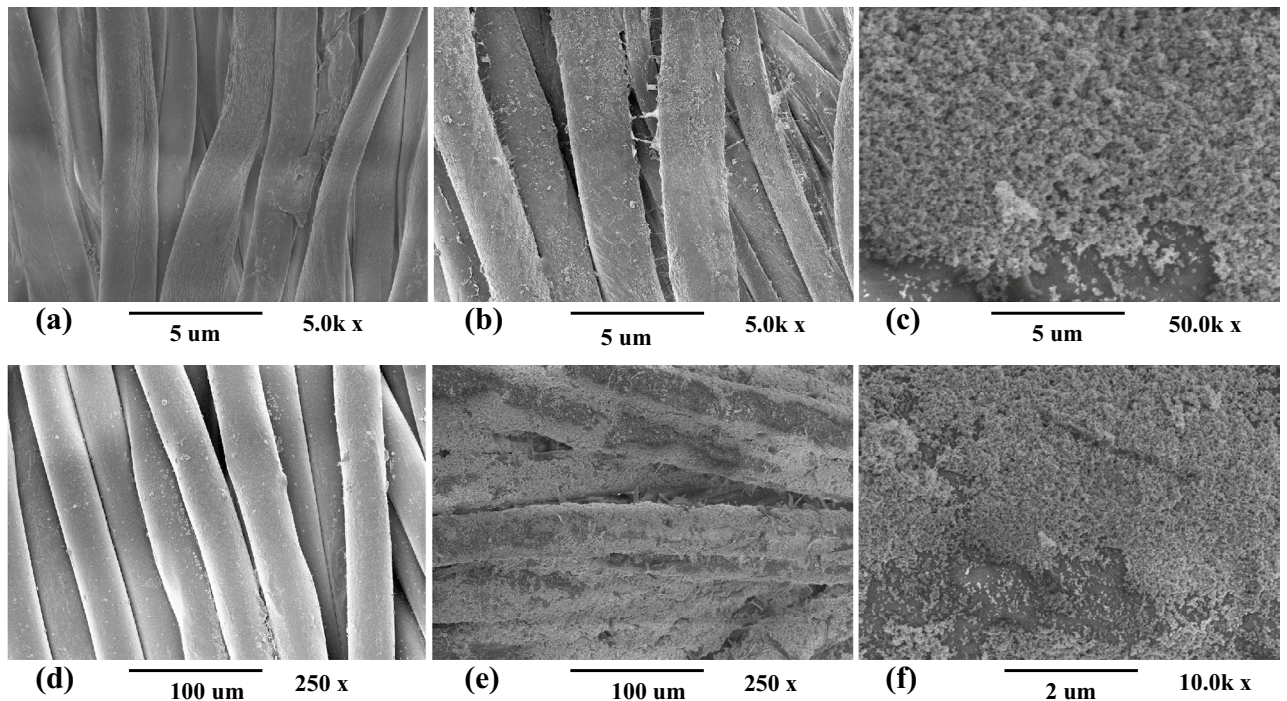


Figure 4. SEM images of (a) untreated cotton fabric, (b) ZnO coated cotton fabric, (c) ZnO coated cotton fabric with higher magnification, (d) untreated polyester fabric, (e) ZnO coated polyester fabric, (f) ZnO coated polyester fabric with higher magnification.

s, in PSO is 0.247 s, in GA is 0.352 s and in CSA is 0.478 s. The average time of each run for heat flow in GEO algorithm is 0.278 s, in PSO is 0.388 s, in GA is 0.421 s and in CSA is 0.762 s. The average time of each run for wetting time in GEO algorithm is 0.178 s, in PSO is 0.265 s, in GA is 0.369 s and in CSA is 0.698 s. The average time of each run for accumulative One-way transport index in GEO algorithm is 0.262 s, in PSO is 0.371 s, in GA is 0.578 s and in CSA is 0.829 s. It is clearly shown that convergence time with GEO is faster than other methods for all predicted properties, that strengthen the accuracy and effectiveness of the proposed ANN-GEO model.

In addition, we applied the conventional MLR method for performance evaluation of ANN-GEO model. The results obtained by MLR are as follows: for thermal resistance MAE=0.7595, MSE=0.739, RMSE=0.8597 and R=0.9676; for thermal diffusivity MAE=0.0075, MSE=0.93787, RMSE=0.0097 and R=0.8007; for heat flow MAE=0.0235, MSE=0.0912, RMSE=0.0302 and R=0.9621; for wetting time MAE=5.6642, MSE=56.3745, RMSE=7.5083 and R=0.8261; and for accumulative One-way transport index MAE=69.1001, MSE=6.23e+03, RMSE=78.9613 and R=0.9447. We observed that the results obtained by ANN-GEO model outperformed MLR for all outputs. The accuracy and the effectiveness of proposed ANN-GEO model is revealed by the obtained results.

For all used optimized models, the performance MSE convergence characteristics have been shown in Fig. 11, where ANN-GEO is in blue, ANN-PSO is in red, ANN-CSA is in red, and ANN-GA is in mauve. We observed that the proposed MLP-GEO model provided the best results with lower MSE values as compared to ANN-PSO, ANN-CSA and ANN-GA for all thermophysiological properties.

Robustness assessment One-way ANOVA was performed to evaluate the effectiveness of predicted results using ANN-GEO, ANN-PSO, ANN-GA, ANN-CSA, ANN, MLR and experiment data. ANOVA is a statistical method aims to determine the correlation between variables and predicted results of ZnO coated fabrics. The results of each comfort property obtained by ANN-GEO, ANN-CSA, ANN-PSO, ANN-GA, ANN, MLR and experimental are illustrated in Table 3. It is observed that ANN-GEO model was more significant as compared to other models as it provide minimum p -value.

Methods	Parameters	Settings
ANN	Training function	Trainlm
	Transfer function of hidden layer	Tansig
	Transfer function of output layer	Purelin
	Hidden node	9
	Input node	3
	Output node	5
	Performance goal	0.00001
	Learning rate	0.02
GEO	Population size	50
	Initial and final attack propensity	[0.5 2]
	Initial and final cruise propensity	[1 0.5]
	Lower and upper bound	[-0.7 0.7]
	Number of iterations	1000
PSO	Population size	50
	Inertia weight	1
	Cognitive factor C1	1.5
	Social factor C2	2
	Random values: r1, r2	[0,1]
	Number of iterations	1000
GA	Population size	50
	Crossover probability	0.4
	Variation probability	0.5
	Crossover method	Float
	Selection method	Roulette method
	Mutation method	Float
	Number of iterations	1000
CSA	Population size	50
	Awareness probability	0.1
	Flight length	2
	Number of iterations	1000

Table 2. Parameters on ANN training network, optimized models with GEO, CSA, PSO, and GA.

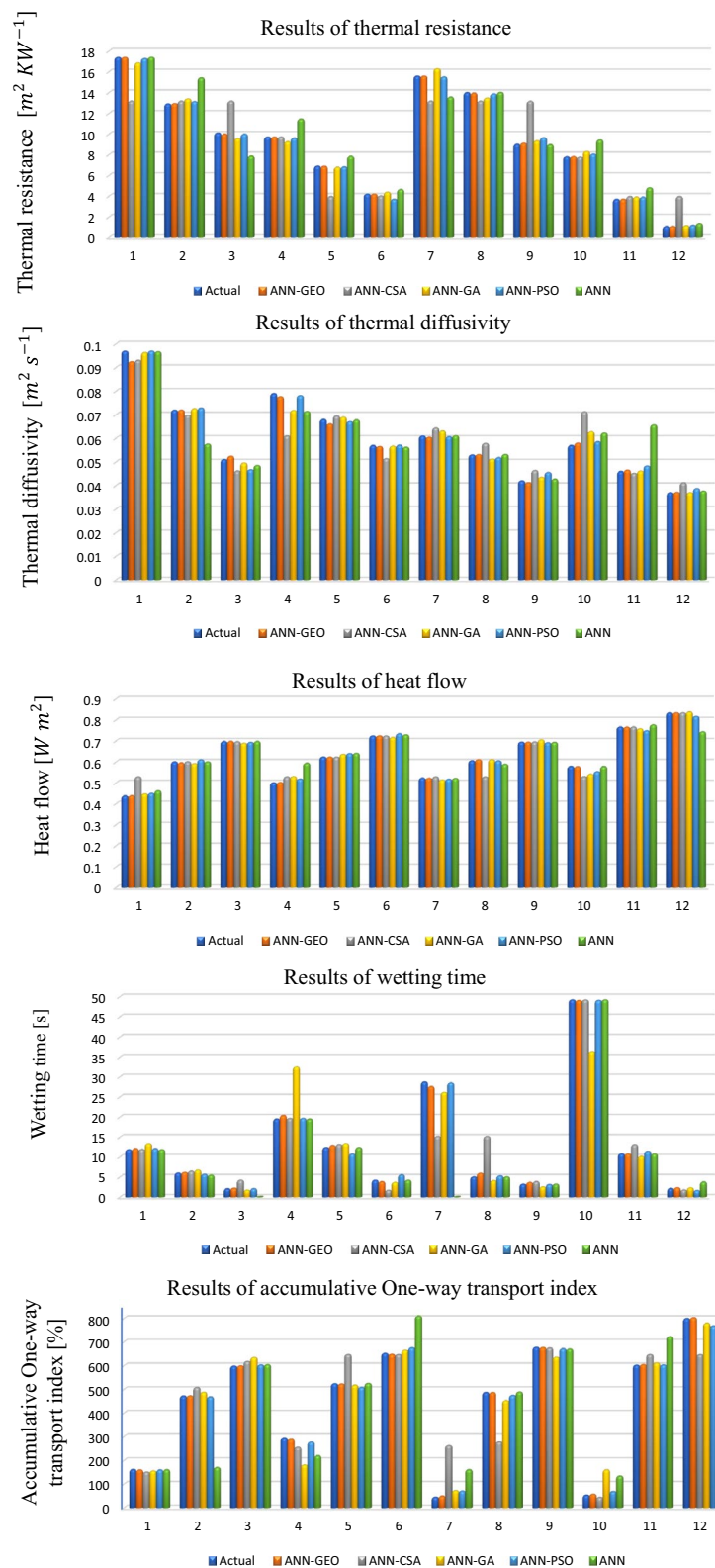


Figure 5. Simulation results for the prediction of thermophysiological comfort properties NPs coated fabrics, where thermal resistance (first row), thermal diffusivity (second row), heat flow (third row), wetting time (fourth row), and accumulative One-way transport index (last row) using ANN-GEO, ANN-CSA, ANN-PSO, ANN-GA and ANN.

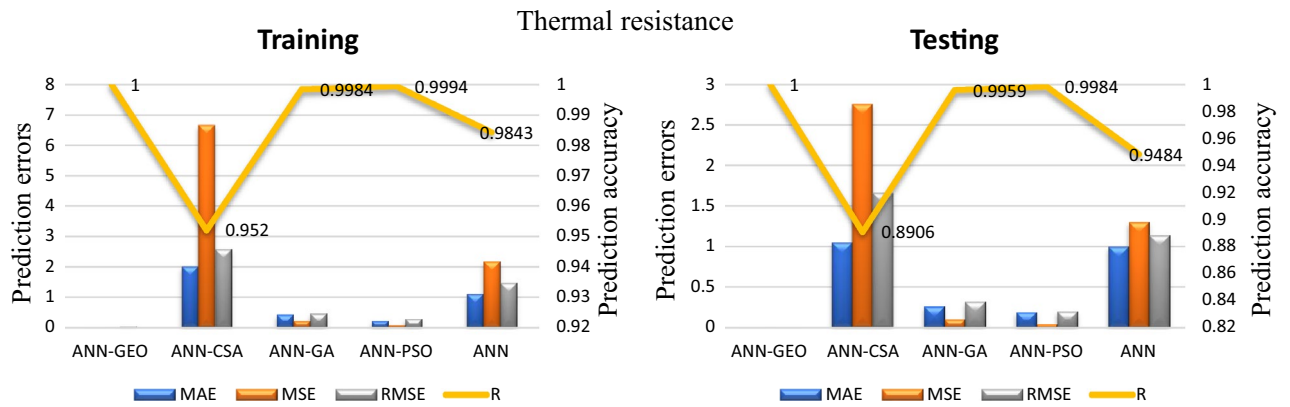


Figure 6. MAE, MSE, RMSE errors, and coefficient of correlation R between predicted and actual values of the thermal resistance using ANN-GEO, ANN-CSA, ANN-PSO, ANN-GA and ANN.

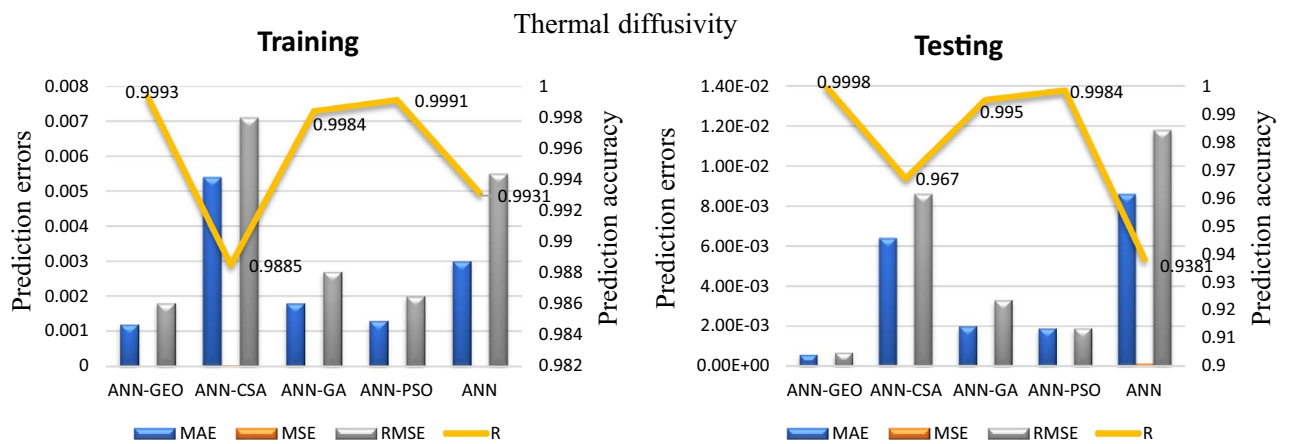


Figure 7. MAE, MSE, RMSE errors, and coefficient of correlation R between predicted and actual values of the thermal diffusivity using ANN-GEO, ANN-CSA, ANN-PSO, ANN-GA and ANN.

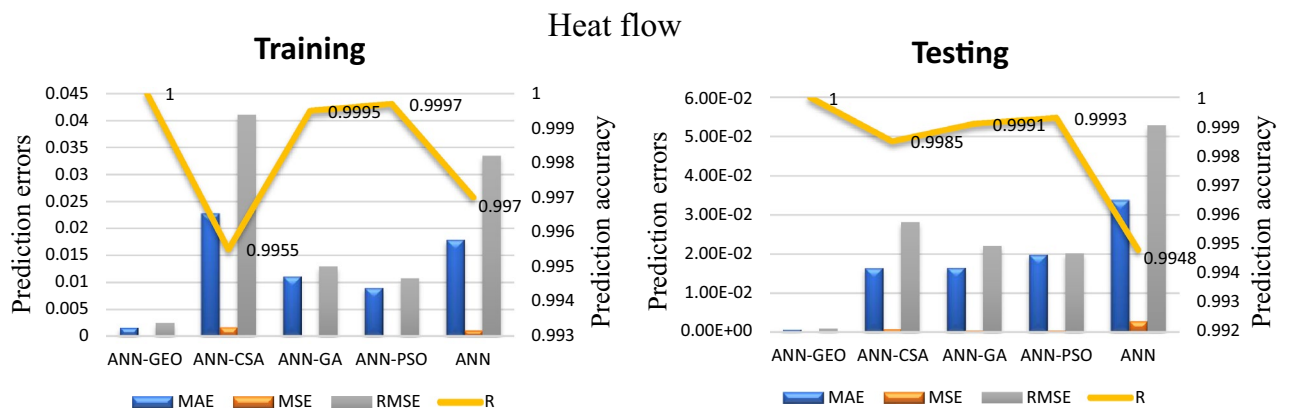


Figure 8. MAE, MSE, RMSE errors, and coefficient of correlation R between predicted and actual values of the heat flow using ANN-GEO, ANN-CSA, ANN-PSO, ANN-GA and ANN.

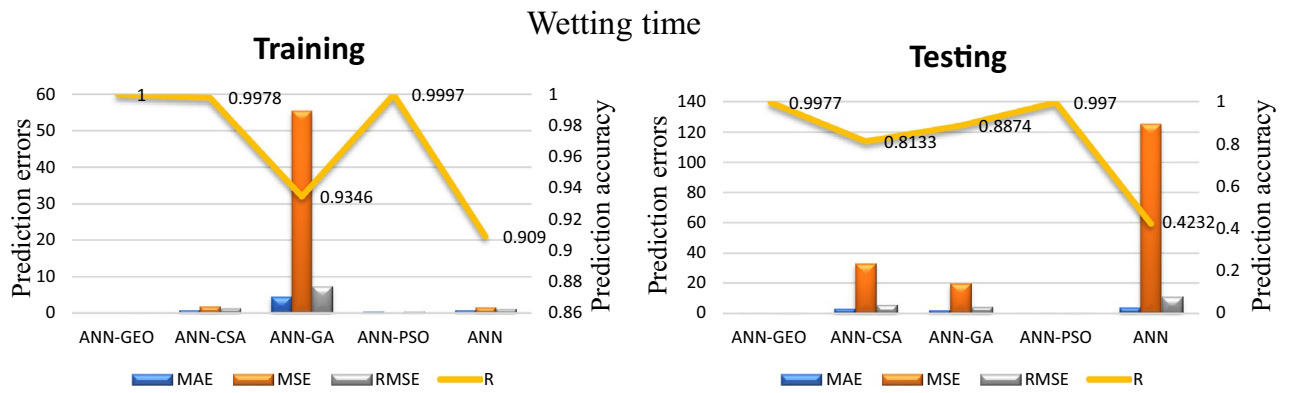


Figure 9. MAE, MSE, RMSE errors, and coefficient of correlation R between predicted and actual values of the wetting time using ANN-GEO, ANN-CSA, ANN-PSO, ANN-GA and ANN.

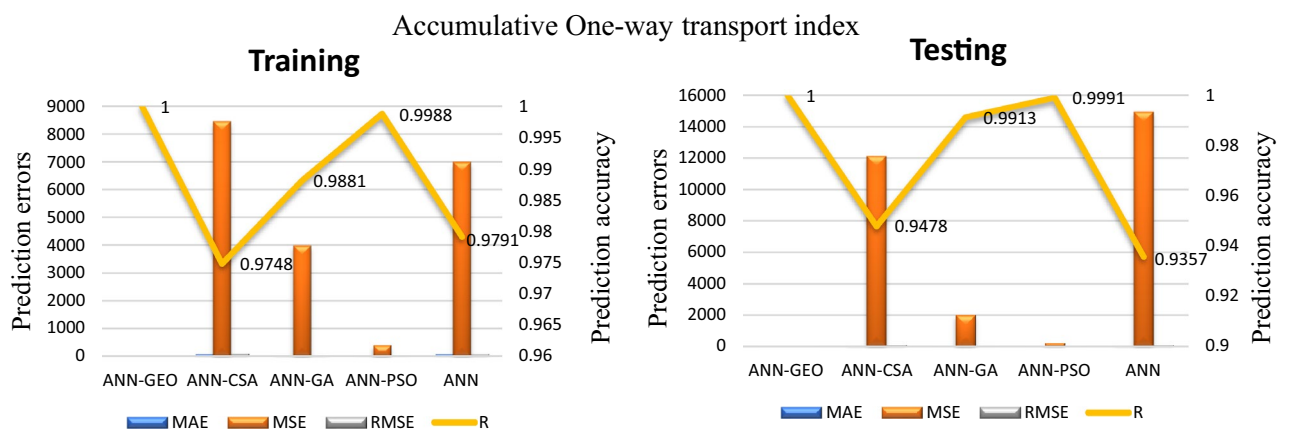


Figure 10. MAE, MSE, RMSE errors, and coefficient of correlation R between predicted and actual values of the accumulative One-way transport index using ANN-GEO, ANN-CSA, ANN-PSO, ANN-GA and ANN.

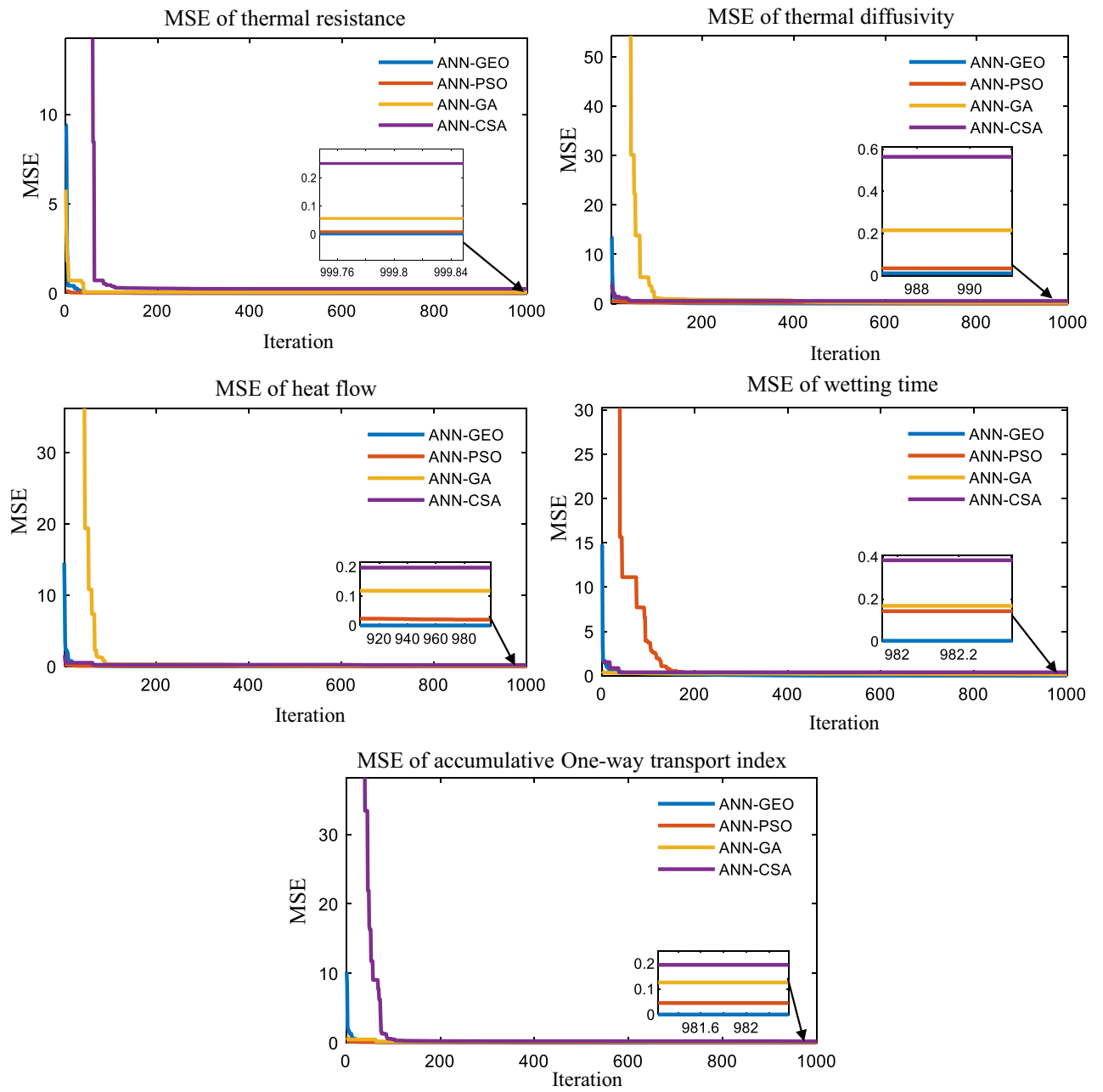


Figure 11. Performance MSE convergence characteristics for ANN-GEO, ANN-CSA, ANN-PSO and ANN-GA.

Thermophysiological comfort properties	Methods	p-value	F-value
Thermal resistance	ANN-GEO	3.22e-07	137.17
	ANN-PSO	8.05e-07	108.55
	ANN-GA	2.28e-06	83.01
	ANN-CSA	0.00016	26.45
	ANN	0.000029	42.52
	MLR	2.67e-6	79.7
	Experimental	2.67e-06	79.66
Thermal diffusivity	ANN-GEO	0.0057	9.18
	ANN-PSO	0.01517	6.53
	ANN-GA	0.0259	5.34
	ANN-CSA	0.0663	3.57
	ANN	0.03174	4.924
	MLR	0.0342	4.72
	Experimental	0.03417	4.77
Heat flow	ANN-GEO	2.91e-06	77.87
	ANN-PSO	5.74e-06	65.27
	ANN-GA	0.000059	35.05
	ANN-CSA	0.0003	21.61
	ANN	0.00026	23.14
	MLR	0.0000728	33.2
	Experimental	0.00007	33.21
Wetting time	ANN-GEO	0.01447	6.65
	ANN-PSO	0.022	5.619
	ANN-GA	0.027	5.20
	ANN-CSA	0.0306	4.99
	ANN	0.030	4.99
	MLR	0.0276	5.21
	Experimental	0.027	5.20
Accumulative One-way transport index	ANN-GEO	0.000024	44.68
	ANN-PSO	0.00011	28.99
	ANN-GA	0.00027	22.87
	ANN-CSA	0.0030	11.27
	ANN	0.00021	24.78
	MLR	0.0003	22.1
	Experimental	0.0003	22.13

Table 3. Analysis report of the predicted values using ANN, ANN-CSA, ANN-PSO, ANN-GA, and ANN-GEO as well as the experimental values for the thermophysiological comfort properties NPs coated fabrics.

Conclusions

In this work, ANN-GEO is introduced as a novel model to enhance the prediction accuracy. ANN-GEO model is a combination of metaheuristics algorithms where GEO is employed for the first time to ameliorate the training process of ANN. ANN-GEO is used for the prediction of thermophysiological comfort of ZnO coated fabrics. The obtained results demonstrated that ANN-GEO model exhibits an efficient prediction accuracy ($R > 99\%$) over standard ANN, ANN-PSO, ANN-CSA, ANN-GA and conventional MLR. Moreover, ANN-GEO showed lower error in terms of MAE, MSE and RMSE. ANN-GEO showed more statistical significant ($p < 0.01147$) than other models. The findings of this study reveal that ANN-GEO can efficaciously be used for prediction as well as for classification of nanocomposites.

Received: 15 December 2021; Accepted: 1 April 2022

Published online: 15 April 2022

References

- Noman, M. T. & Petru, M. Functional properties of sonochemically synthesized zinc oxide nanoparticles and cotton composites. *Nanomaterials* <https://doi.org/10.3390/nano10091661> (2020).
- Dong, S. *et al.* A novel and high-performance double Z-scheme photocatalyst ZnO-SnO₂-Zn₂SnO₄ for effective removal of the biological toxicity of antibiotics. *J. Hazard. Mater.* **399**, 123017. <https://doi.org/10.1016/j.jhazmat.2020.123017> (2020).
- Noman, M. T., Amor, N., Petru, M., Mahmood, A. & Kejzlar, P. Photocatalytic behaviour of zinc oxide nanostructures on surface activation of polymeric fibres. *Polymers* <https://doi.org/10.3390/polym13081227> (2021).

4. Noman, M. T., Petru, M., Amor, N. & Louda, P. Thermophysiological comfort of zinc oxide nanoparticles coated woven fabrics. *Sci. Rep.* <https://doi.org/10.1038/s41598-020-78305-2> (2020).
5. Noman, M., Petru, M., Louda, P. & Kejzlar, P. Woven textiles coated with zinc oxide nanoparticles and their thermophysiological comfort properties. *J. Nat. Fibers* **18**, 1–14. <https://doi.org/10.1080/15440478.2020.1870621> (2021).
6. Amor, N., Noman, M. T., Ismail, A., Petru, M. & Neethu, S. Use of an artificial neural network for tensile strength prediction of nano titanium dioxide coated cotton. *Polymers* <https://doi.org/10.3390/polym14050937> (2022).
7. Azeem, M., Noman, M. T., Wiener, J., Petru, M. & Louda, P. Structural design of efficient fog collectors: A review. *Environ. Technol. Innov.* **20**, 101169. <https://doi.org/10.1016/j.eti.2020.101169> (2020).
8. Noman, M. T., Petru, M., Militky, J., Azeem, M. & Ashraf, M. A. One-pot sonochemical synthesis of ZnO nanoparticles for photocatalytic applications, modelling and optimization. *Materials* <https://doi.org/10.3390/ma13010014> (2020).
9. Khude, P., Majumdar, A. & Butola, B. S. Modelling and prediction of antibacterial activity of knitted fabrics made from silver nanocomposite fibres using soft computing approaches. *Neural Comput. Appl.* **32**, 9509–9519 (2019).
10. Kanat, Z. E. & Özdil, N. Application of artificial neural network (ANN) for the prediction of thermal resistance of knitted fabrics at different moisture content. *J. Text. Inst.* **109**, 1247–1253. <https://doi.org/10.1080/00405000.2017.1423003> (2018).
11. Lu, D. & Yu, W. Predicting the tensile strength of single wool fibers using artificial neural network and multiple linear regression models based on acoustic emission. *Text. Res. J.* **91**, 533–542. <https://doi.org/10.1177/0040517520948200> (2021).
12. Malik, S. A. *et al.* Analysis and prediction of air permeability of woven barrier fabrics with respect to material, fabric construction and process parameters. *Fibers Polym.* **18**, 2005–2017 (2017).
13. Malik, S. A., Kocaman, R. T., Gereke, T., Aibibu, D. & Cherif, C. Prediction of the porosity of barrier woven fabrics with respect to material, construction and processing parameters and its relation with air permeability. *Fibres Text. Eastern Eur.* **26**, 71–79 (2018).
14. Wong, A., Li, Y. & Yeung, P. Predicting clothing sensory comfort with artificial intelligence hybrid models. *Text. Res. J.* **74**, 13–19. <https://doi.org/10.1177/004051750407400103> (2004).
15. Mishra, S. Prediction of yarn strength utilization in cotton woven fabrics using artificial neural network. *J. Inst. Eng. (India) Ser. E* **96**, 151–157 (2015).
16. El-Geiheini, A., ElKateb, S. & Abd-Elhamied, M. R. Yarn tensile properties modeling using artificial intelligence. *Alex. Eng. J.* **59**, 4435–4440. <https://doi.org/10.1016/j.aej.2020.07.049> (2020).
17. Erbil, Y., Babaarslan, O. & Ilhami, Ilhan. A comparative prediction for tensile properties of ternary blended open-end rotor yarns using regression and neural network models. *J. Text. Inst.* **109**, 560–568. <https://doi.org/10.1080/00405000.2017.1361164> (2018).
18. Breuer, K. & Stommel, M. Prediction of short fiber composite properties by an artificial neural network trained on an rve database. *Fibers* <https://doi.org/10.3390/fib9020008> (2021).
19. Wang, F. *et al.* A model for predicting the tensile strength of ultrafine glass fiber felts with mathematics and artificial neural network. *J. Text. Inst.* **112**, 783–791. <https://doi.org/10.1080/00405000.2020.1779167> (2021).
20. Farooq, A. *et al.* Predicting cotton fibre maturity by using artificial neural network. *Autex Res. J.* **18**, 429–433 (2018).
21. Unal, P., Üreyen, M. & Mecit, D. Predicting properties of single jersey fabrics using regression and artificial neural network models. *Fibers Polym.* **13**, 87–95 (2012).
22. Farooq, A., Irshad, F., Azeemi, R. & Iqbal, N. Prognosticating the shade change after softener application using artificial neural networks. *Autex Res. J.* <https://doi.org/10.2478/aut-2020-0019> (2020).
23. Amor, N., Noman, M. T. & Petru, M. Prediction of functional properties of nano TiO₂ coated cotton composites by artificial neural network. *Sci. Rep.* <https://doi.org/10.1038/s41598-021-91733-y> (2021).
24. Amor, N., Noman, M. T. & Petru, M. Prediction of methylene blue removal by nano TiO₂ using deep neural network. *Polymer* <https://doi.org/10.3390/polym13183104> (2021).
25. Malik, S. A., Gereke, T., Farooq, A., Aibibu, D. & Cherif, C. Prediction of yarn crimp in pes multifilament woven barrier fabrics using artificial neural network. *J. Text. Inst.* **109**, 942–951 (2018).
26. Xiao, Q. *et al.* Prediction of pilling of polyester-cotton blended woven fabric using artificial neural network models. *J. Eng. Fibers Fabr.* <https://doi.org/10.1177/1558925019900152> (2020).
27. Dashedi, M., Derhami, V. & Ekhtiyari, E. Yarn tenacity modeling using artificial neural networks and development of a decision support system based on genetic algorithms. *J. AI Data Min.* **2**, 73–78. <https://doi.org/10.22044/jadm.2014.187> (2014).
28. Majumdar, A., Das, A., Hatua, P. & Ghosh, A. Optimization of woven fabric parameters for ultraviolet radiation protection and comfort using artificial neural network and genetic algorithm. *Neural Comput. Appl.* **27**, 2567–2576. <https://doi.org/10.1007/s00521-015-2025-6> (2016).
29. Ni, C. *et al.* Online sorting of the film on cotton based on deep learning and hyperspectral imaging. *IEEE Access* **8**, 93028–93038 (2020).
30. Lazzús, J. A. Neural network-particle swarm modeling to predict thermal properties. *Math. Comput. Modell.* **57**, 2408–2418. <https://doi.org/10.1016/j.mcm.2012.01.003> (2013).
31. Amor, N., Noman, M. T., Petru, M., Mahmood, A. & Ismail, A. Neural network-crow search model for the prediction of functional properties of nano TiO₂ coated cotton composites. *Sci. Rep.* <https://doi.org/10.1038/s41598-021-93108-9> (2021).
32. Mohammadi-Balani, A., Dehghan Nayeri, M., Azar, A. & Taghizadeh-Yazdi, M. Golden eagle optimizer: a nature-inspired metaheuristic algorithm. *Comput. Ind. Eng.* **152**, 107050. <https://doi.org/10.1016/j.cie.2020.107050> (2021).
33. Noman, M. T. *et al.* Sonochemical synthesis of highly crystalline photocatalyst for industrial applications. *Ultrasonics* **83**, 203–213. <https://doi.org/10.1016/j.ultras.2017.06.012> (2018).
34. Noman, M. T. *et al.* In-situ development of highly photocatalytic multifunctional nanocomposites by ultrasonic acoustic method. *Ultrason. Sonochem.* **40**(Pt A), 41–56. <https://doi.org/10.1016/j.ultsonch.2017.06.026> (2018).
35. Amor, N., Noman, M. T. & Petru, M. Classification of textile polymer composites: Recent trends and challenges. *Polymers* <https://doi.org/10.3390/polym13162592> (2021).
36. Pishro, A. A. *et al.* Application of artificial neural networks and multiple linear regression on local bond stress equation of uhpc and reinforcing steel bars. *Sci. Rep.* **11** (2021).
37. Wang, Z., Di Massimo, C., Tham, M. T. & Julian Morris, A. A procedure for determining the topology of multilayer feedforward neural networks. *Neural Netw.* **7**, 291–300. [https://doi.org/10.1016/0893-6080\(94\)90023-X](https://doi.org/10.1016/0893-6080(94)90023-X) (1994).
38. Kalantary, S., Jahani, A. & Jahani, R. Mlr and ann approaches for prediction of synthetic/natural nanofibers diameter in the environmental and medical applications. *Sci. Rep.* **10** (2020).
39. Jeon, J. H., Yang, S. S. & Kang, Y. J. Estimation of sound absorption coefficient of layered fibrous material using artificial neural networks. *Appl. Acoust.* **169**, 107476. <https://doi.org/10.1016/j.apacoust.2020.107476> (2020).
40. Doran, E. C. & Sahin, C. The prediction of quality characteristics of cotton/elastane core yarn using artificial neural networks and support vector machines. *Text. Res. J.* **90**, 1558–1580. <https://doi.org/10.1177/0040517519896761> (2020).
41. Daniel, G. G. *Artificial Neural Network*, 143–143 (Springer, Netherlands, Dordrecht, 2013).
42. Briot, J.-P. From artificial neural networks to deep learning for music generation: history, concepts and trends. *Neural Comput. Appl.* **33**, 39–65. <https://doi.org/10.1007/s00521-020-05399-0> (2021).
43. Ayres, L., Gomez, F., Linton, J., Silva, M. & Garcia, C. Taking the leap between analytical chemistry and artificial intelligence: A tutorial review. *Anal. Chim. Acta* <https://doi.org/10.1016/j.aca.2021.338403> (2021).
44. Jain, A. K., Jianchang, Mao & Mohiuddin, K. M. Artificial neural networks: a tutorial. *Computer* **29**, 31–44. <https://doi.org/10.1109/2.485891> (1996).

45. Golnaraghi, S., Zangenehmadar, Z., Moselhi, O. & Alkass, S. Application of artificial neural network(s) in predicting formwork labour productivity. *Adv. Civ. Eng.* **2019**, 1–11 (2019).
46. Rezaee, M. J., Jozmaleki, M. & Valipour, M. Integrating dynamic fuzzy C-means, data envelopment analysis and artificial neural network to online prediction performance of companies in stock exchange. *Phys. A Stat. Mech. Appl.* <https://doi.org/10.1016/j.physa.2017.07.017> (2018).
47. Das, S., Ghosh, A., Majumdar, A. & Banerjee, D. Yarn engineering using hybrid artificial neural network-genetic algorithm model. *Fibers Polym.* **14**, 1220–1226 (2013).
48. Ecer, F., Ardabili, S., Band, S. S. & Mosavi, A. Training multilayer perceptron with genetic algorithms and particle swarm optimization for modeling stock price index prediction. *Entropy* <https://doi.org/10.3390/e22111239> (2020).
49. Ansari, A., Ahmad, I. S., Bakar, A. A. & Yaakub, M. R. A hybrid metaheuristic method in training artificial neural network for bankruptcy prediction. *IEEE Access* **8**, 176640–176650. <https://doi.org/10.1109/ACCESS.2020.3026529> (2020).
50. Ram Jethmalani, C. H., Simon, S. P., Sundareswaran, K., Nayak, P. S. R. & Padhy, N. P. Auxiliary hybrid PSO-BPNN-based transmission system loss estimation in generation scheduling. *IEEE Trans. Ind. Inf.* **13**, 1692–1703. <https://doi.org/10.1109/TII.2016.2614659> (2017).
51. Noman, M. T., Amor, N. & Petru, M. Synthesis and applications of ZnO nanostructures (ZONs): a review. *Crit. Rev. Solid State Mater. Sci.* **2**, 1–44. <https://doi.org/10.1080/10408436.2021.1886041> (2021).
52. Balram, D., Lian, K. Y., Sebastian, N., Mahmood, F. S. & Noman, M. T. Ultrasensitive detection of food colorant sunset yellow using nickel nanoparticles promoted lettuce-like spinel Co₃O₄ anchored GO nanosheets. *Food Chem. Toxicol.* **159**, 112725. <https://doi.org/10.1016/j.fct.2021.112725> (2022).
53. Sebastian, N., Yu, W. C., Balram, D., Mahmood, F. S. & Noman, M. T. Functionalization of CNFs surface with β -cyclodextrin and decoration of hematite nanoparticles for detection and degradation of toxic fungicide carbendazim. *Appl. Surf. Sci.* **586**, 152666. <https://doi.org/10.1016/j.apsusc.2022.152666> (2022).

Acknowledgements

This work was supported by the Ministry of Education, Youth and Sports of the Czech Republic and the European Union (European Structural and Investment Funds-Operational Programme Research, Development and Education) in the frames of the project “Modular platform for autonomous chassis of specialized electric vehicles for freight and equipment transportation”, Reg. No. CZ.02.1.01/0.0/0.0/16–025/0007293.

Author contributions

N. A. and M.T.N. conceived, designed and performed experiments; analysed the results and wrote manuscript. N.S. analysed the results and wrote manuscript. M. P. analyzed the results, supervised and acquired funding. All of the authors participated in critical analysis and preparation of the manuscript.

Competing interests

The authors declare no competing interests.

Additional information

Correspondence and requests for materials should be addressed to N.A.

Reprints and permissions information is available at www.nature.com/reprints.

Publisher’s note Springer Nature remains neutral with regard to jurisdictional claims in published maps and institutional affiliations.



Open Access This article is licensed under a Creative Commons Attribution 4.0 International License, which permits use, sharing, adaptation, distribution and reproduction in any medium or format, as long as you give appropriate credit to the original author(s) and the source, provide a link to the Creative Commons licence, and indicate if changes were made. The images or other third party material in this article are included in the article’s Creative Commons licence, unless indicated otherwise in a credit line to the material. If material is not included in the article’s Creative Commons licence and your intended use is not permitted by statutory regulation or exceeds the permitted use, you will need to obtain permission directly from the copyright holder. To view a copy of this licence, visit <http://creativecommons.org/licenses/by/4.0/>.

© The Author(s) 2022